Evolution of Secondary Marigold Flower Waste as Electrode for Zinc-Based Hybrid Supercapacitor

[a] *Sayli Pradhan,* [b]*Umer Khan,* [b]*Jyotsna T. Waghmare,* [*a] *Neetu Jha*

nan19.sr.pradhan@pg.ictmumbai.edu.in

nr.jha@ictmumbai.edu.in

[*a] Department of Physics, Institute of Chemical Technology, Mumbai 400019, India

[b] Department of Oils, Oleochemicals and Surfactants, Institute of Chemical Technology, Mumbai, 400019, India

Abstract:

In this study, secondary marigold flowers waste (SMW) was successfully converted into porous carbons through hydrothermal carbonization (HTC) followed by pyrolysis. The high-temperature pyrolysis led to the complete removal of functional groups due to dehydration and decarboxylation processes. The resulting hierarchical porous carbon material (HPCM), when employed as the positive electrode in a zinc-ion hybrid supercapacitor (ZBHSC), exhibited a specific capacity of 157.44 mAh g^{-1} at a current density of 0.3 A g^{-1}. The ZBHSC incorporating HPCM as the positive electrode maintained a capacity retention of 71.57% and a coulombic efficiency of 90.17% over 200 cycles. The developed ZBHSC achieved an impressive balance between energy and power, with a peak energy density of 56 Wh kg^{-1} at 106 W kg^{-1} and a high-power density of 1.07 kW kg^{-1} at 4.18 Wh kg^{-1}. These results underscore the potential of HPCM derived from SMW as a versatile material for advanced energy storage applications.

Keywords: *Marigold flower, secondary waste material, hydrothermal carbonization, Zinc based hybrid supercapacitor, hydrothermally carbonized Marigold, and hydro-pyro-carbonization of Marigold.*

1. Introduction

Fossil fuel consumption causes air pollution and contributes to global warming. Fossil fuel distribution and extraction also have an impact on the environment and add to the cost of protecting a country against local fossil fuel shortages[1]. Modern electric vehicle technology and large-scale grid energy storage, among other things, have made the need for sophisticated energy storage systems that are highly effective, affordable, and environmentally benign more pressing [2-4]. Batteries and supercapacitors, which are now used for commercial energy storage, can't accommodate all of the needs for energy storage in the future. Applications for lithium-ion batteries (LIBs) are hampered by their low power density, scarcity of lithium resource materials, poor cycling stability, and safety [5]. Moreover, the low energy density of supercapacitors prevents their use in many applications [6] . The development of new electrochemical hybrid supercapacitors, which combine the benefits of batteries and supercapacitors, has drawn significant interest and become an important research topic in the field of energy storage [6-11].

Several metal-ion hybrid supercapacitors, including Li, Na, and Zn, have drawn a lot of attention in recent years. Zinc based hybrid supercapacitors (ZBHSC), which consist of one electrode that is similar to a battery (Zn) and one electrode that is similar to a capacitor (carbon based). In aqueous system, the Zn metal can easily strip or plate charge-carrying cations when used as an anode[12]. In fact, the development of improved metal-ion hybrid supercapacitors depends heavily on this design approach[13]. In mild neutral electrolytes as $ZnSO_4$, the Zn-ion hybrid supercapacitor exhibits a number of noteworthy benefits, including good safety, an ample Zn resource, low cost, and a chemically inert,

low toxicity [14,15]. The zinc anode has a higher theoretical capacity (5854 mA h cm^{-3} and 820 mA h g^{-1}) than the market-leading lead-acid batteries and a comparatively low redox potential (-0.76 V vs standard hydrogen electrode) [16-19]. For real-time application, the development of electrochemically efficient, low-cost, high surface area, and highly stable positive electrode is desired for ZBHSC application.

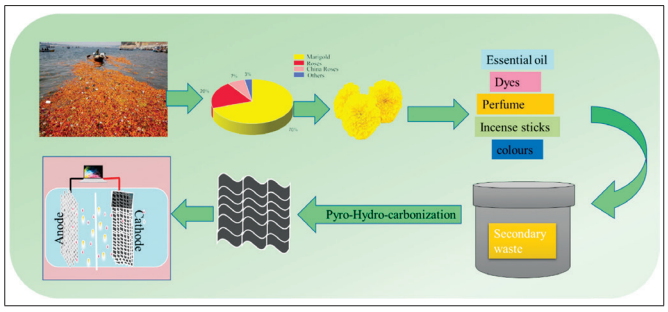


Fig. 1:Evolution of secondary Marigold waste

Marigold flowers are utilised in religious places, where they are offered to deities and used for decoration before being abandoned and becoming garbage [20]. After offering the florals to the deities, the flowers serve their purpose of worship but lose their value and are then treated as rubbish, collected with other waste before being deposited in water bodies or with other waste, polluting the environment. Marigold floral waste (MFW) has a low pH and is high in micronutrients (Fe, Mn, Zn, Cu, and so on) as well as macronutrients (N, P, K, and Ca) [21]. The nutrient richness of MFW causes eutrophication of water bodies, resulting in the extinction of aquatic fauna. This primary floral waste can be used to make a variety of small-scale goods like perfumes, essential oils, dyes, incense sticks, and colours, etc. [22]. This can be referred to as primary waste recycling. The primary recycling industries or laboratories generates residual waste after processing primary waste which termed as secondary Marigold waste (SMW). It is essential to address SMW as degrading flower releases toxic gases such as methane (CH_4), carbon dioxide (CO_2), ammonia (NH_3), and others, which generate a terrible odour when dumped in the open [23]. To grow flower, a variety of chemical fertilisers are utilised, so leachate from decomposing waste can seep the ground and contaminate groundwater. As a result, improper management of secondary waste material (SMW) from industries or laboratories may leads to air, water, and soil pollution [24].

Hence, after investigated whether it was possible to use these SMW and turn them into something with more worth. It is found that chemically cellulose, hemicellulose, and lignin make up the majority of SMW [25]. Plant biomass' lignocellulosic structure is widely known as a significant carbon source for the creation of porous carbon composites[26-28]. Recently, attention has been drawn to porous carbon as an intriguing material for a variety of uses, such as electrode material in electrochemical devices[28], [29]. Due to the ongoing decline in the supply of fossil fuels, the use of carbon compounds obtained from waste or biomass has recently become exciting for a variety of applications, notably for energy storage[30].

Numerous researchers have reported that high surface area activated carbon with excellent energy storage capabilities can be made from a variety of sources, including lotus pollen[31], sunflower seeds [32], silk protein [33], watermelon [34], hemp [35], cow dung [36], oil palm[37], yoghurt [38], eggshell membrane [39], coffee beans [40], human hairs [41], and others. The majority of these materials are unusual and tricky to locate. It would therefore be beneficial and more useful if activated carbon could be made from inexpensive, abundant, but discarded materials like SWM. Plant biomass can be transformed into products with a high carbon content using the thermochemical process known as hydrothermal carbonization (HTC)[42-44].

Here, the recycling of most ignored secondary waste is carried out to derive porous carbon for energy storage application without any residual waste. The evolution of Marigold flower to porous carbon can be seen in fig. 1. The HTC and pyrolysis techniques were employed to synthesize porous carbons using SMW as a precursor. Both temperature and time used in HTC strongly affect physical and chemical properties as well as porous structure. The carbon produced has an amorphous phase. The prospect of

using microporous carbons made from discarded SMW as positive electrode materials in ZBHSC is investigated using various characterization techniques.

2. Experimental Section

2.1. Synthesis of material

The Secondary marigold floral waste was collected from the oils and dye laboratory where marigold waste was used for extracting oils and dye. The secondary waste is washed with DI water and dried in a hot oven at 80 °C for 30 h. Later, for hydrothermal carbonization (HTC), 20 g of dried secondary marigold material with 100 ml of DI water loaded in a Teflon-lined stainless-steel autoclave and HTC was performed at 190 °C for 24 h. The obtained hydrochar was washed and dried. The collected product designated as hydrothermally carbonized Marigold (HCM). Then following pyrolysis process was carried out in a tube furnace at 800 °C for 1 h with a heating rate of 10 °C/min under Argon (Ar) gas flow (0.3 L/min). The resultant product was crushed into a fine powder using a mortar and pestle. The obtained product named as hydro-pyro-carbonized Marigold (HPCM) to be implied as positive electrode for hybrid supercapacitor.

2.2. Electrochemical characterization

To understand electrochemical behaviour of HPCM material as cathode in hybrid supercapacitor system, a suspension of 10 mg of HPCM in DI water (10 ml) was sonicated for 1 hour in a bath sonicator. The HPCM slurry was then spin coated on carbon paper and dried for 12 hours in a furnace at 80°C. Glass fibre membrane was used as a separator, zinc foil (0.25 mm thickness) was used as an anode, and 2M $ZnSO_4$ was used as the electrolyte for ZIBs to examine the electrochemical properties of HPCM as a cathode for ZIBs. With a NOVA (Metrohm AUTOLAB) potentiostat galvanostat on a Metrohm (PGSTAT 204) electrochemical impedance spectroscopy (EIS), galvanostatic charge-discharge (GCD), and cyclic voltammetry (CV) measurements were studied.

1.3. Material characterization

The structure of HPCM was investigated using X-ray Diffraction (Bruker D8 Advance, Bruker, Germany) with Cu K-α radiation (k =1.54 Å) and a scanning range of 10-80˚ is maintained. Raman spectrum analysis was performed using an argon ion to excite a confocal LabRAM HR800 spectrometer (Horiba Jobin-Yvon, France.) with an excitation wavelength of 532 nm and a wavenumber range of 500-2500 cm^{-1} for HPCM. The surface area measurements were carried out using Brunauer–Emmett–Teller (BET) (BELSORP-miniX, Microtrac, Japan). The field emission scanning electron microscopy (FESEM) and energy dispersive X-ray analysis (EDX) (Supra 55, Carl Zeiss, Germany) were performed for HCM and HPCM.

3. Results and discussion

3.1 Material characterization

The X-ray diffraction pattern (XRD) of HCM and HPCM is shown in Fig.2(a), Two broad peaks in the XRD can be seen for hydrocarbonized secondary marigold waste before and after pyrolysis at 25.63° and 43.41°, which are reflections from planes (002) and (101), respectively. These peaks suggest material has hexagonal graphitic structure [45], [46]. Remarkably, there are small yet important differences in the intensity of the major peak around 25.63°. With pyrolysis, a sharper peak is apparent in the XRD for HPCM sample synthesized in this study. Raman spectra (Fig. 2(b)) reveal details on molecular vibrations and the composition of the material. It is commonly used to describe carbonaceous materials' structural characteristics. The peaks at 1347 and 1591 cm^{-1} denote D and G bands of carbon, respectively. The G band relates to the vibration of sp^2 linked atoms in a two-dimensional hexagonal lattice, while the D band is attributed to defects. The degree of graphitization is calculated using the peak intensity ratios of the D and G band, represented as I_D/I_G. The I_D/I_G ratio is 0.33 for HCM while after annealing at 800˚ C, the I_D/I_G ratio is 1.06 for HPCM material, which suggests the presence of a disordered carbon matrix.

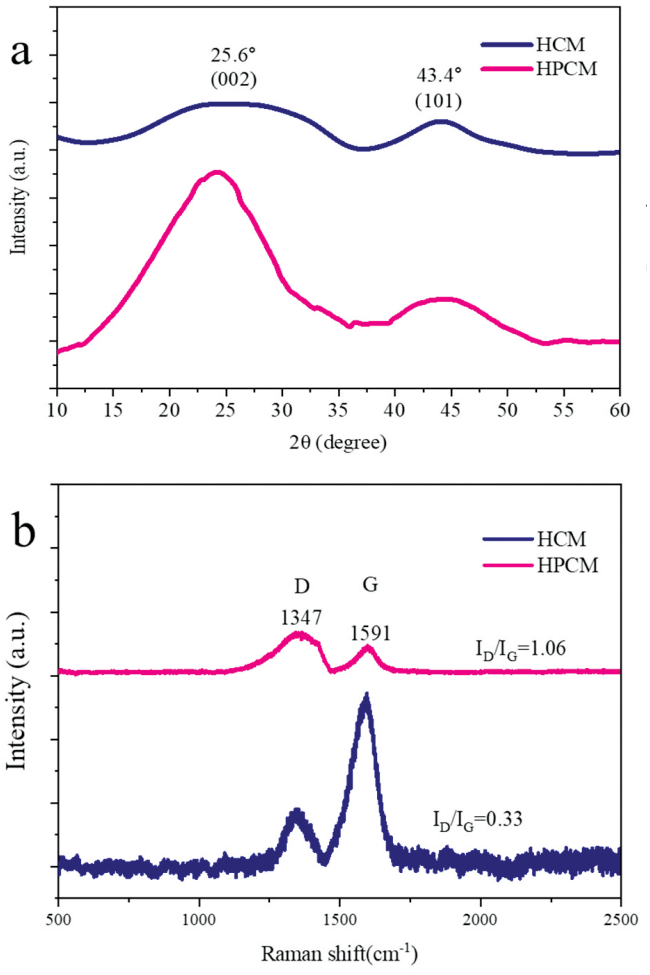


Fig. 2a) XRD pattern and b) Raman spectras for HCM and HPCM

The BET analysis is a crucial characterization technique used to evaluate the specific surface area and porosity of materials, which are essential properties influencing their performance in various applications, including catalysis, adsorption, and energy storage. In this study, BET adsorption and desorption measurements were conducted using nitrogen (N_2) as the adsorbate to investigate the surface characteristics of materials HCM and HPCM shown fig. 3(a). HPCM exhibits a significantly higher BET surface area of 258 m²/g, nearly 175 times greater than that of HCM (1.47 m²/g). Fig. 3(b) shows the pore size distribution for HCM and HPCM. It can be noted that extensive surface area of HPCM is complemented by an optimal average pore size of 2.3 nm, which, along with the diverse range of pores, enhances its ability to accommodate Zn ions and electrolyte.

In comparison, material HCM, with an average pore size of 2.9 nm, offers a slightly larger pore structure but with a considerably lower surface area. While the larger pores in HCM material may benefit applications requiring more straightforward diffusion pathways, its limited surface area reduces the number of active sites available for surface interactions. This makes HCM less effective in applications where high surface area and optimal pore size distribution are critical. The varied pore sizes in HPCM facilitate efficient ion diffusion and storage, making it particularly suitable for energy storage applications such as batteries and supercapacitors. Therefore, due to its combination of high surface area and a more favourable pore size distribution, HPCM material is more suitable for energy storage applications.

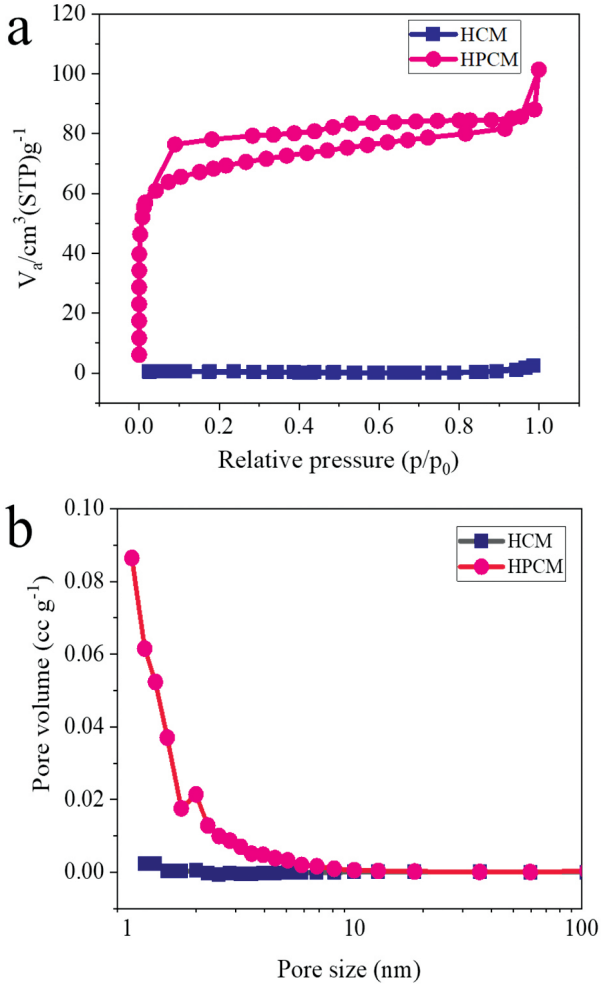


Fig. 3.a) BET surface area adsorption-desorption isotherm of CF with all prepared ratios in N^2 atmosphere at 77 k. a) Pore size distribution

The FESEM was conducted to investigate the surface morphology and structural characteristics of HCM and HPCM materials. The FESEM images reveal distinct differences between the two samples, particularly in their surface textures and pore structures. In fig. 4(a), HCM exhibits a relatively smooth surface with few visible pores, indicating a more compact and less porous structure. The surface morphology suggests that HCM may have a lower surface area, consistent with the BET analysis, which showed a smaller specific surface area. The uniformity in the surface structure of HCM indicates fewer surface defects, which could influence its performance in applications requiring minimal surface reactivity. In contrast, HPCM displays a much more complex and heterogeneous surface morphology. The FESEM images fig 4(b) show that HPCM has undergone carbonization, possesses a network of pores of varying sizes distributed across its surface. This porous structure is characteristic of carbonized lignocellulose, suggesting that HPCM retains the fibrous and hierarchical structure of its precursor material. The carbonization process appears to have enhanced the surface roughness and created a diverse pore structure, contributing to the higher surface area observed in the BET analysis. The presence of different sizes of pores indicates that HPCM can offer superior performance in applications requiring high surface interactions, such as energy storage or catalysis, where a well-developed porous network is advantageous.

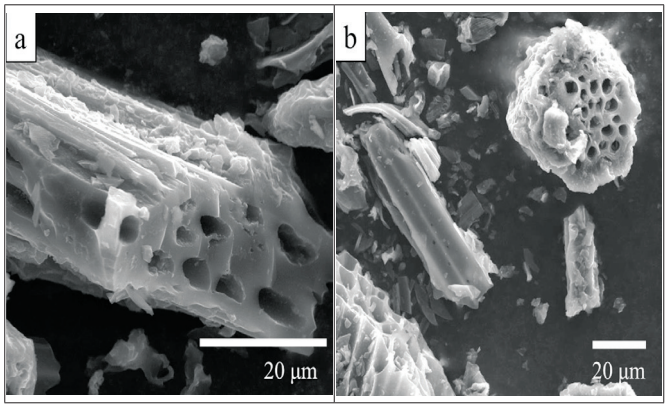


Fig. 4.FESEM images at 20 µm scale a) HCM and b) HPCM

3.2 Electrochemical characterization

In order to analyse the entire electrochemical response of the electrode material, including the charge holding capacity and charge storage behaviour, electrochemical analysis is crucial. To study the electrochemical response of zinc-based hybrid supercapacitor (ZBHSC) using HPCM as positive electrode, zinc foil as negative electrode and 2M $ZnSO_4$ as electrolyte in Swagelok cell was used. Fig. 5 shows the illustration of reaction mechanism for hybrid supercapacitor. Reversible ion adsorption/desorption on HPCM cathode and Zn (Zn^{2+}) deposition/stripping on Zn anode enable the ZBHSC to repeatedly store/deliver electrical energy.

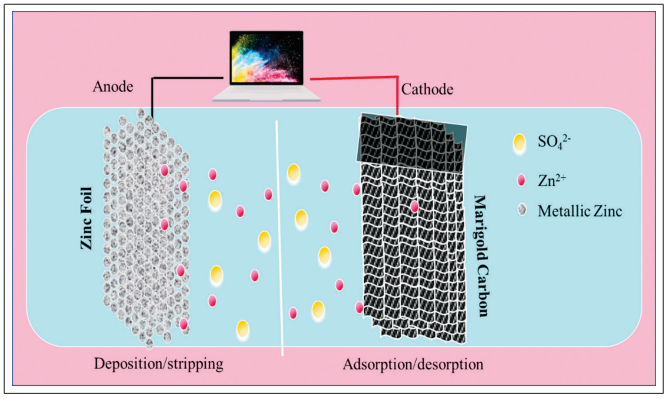
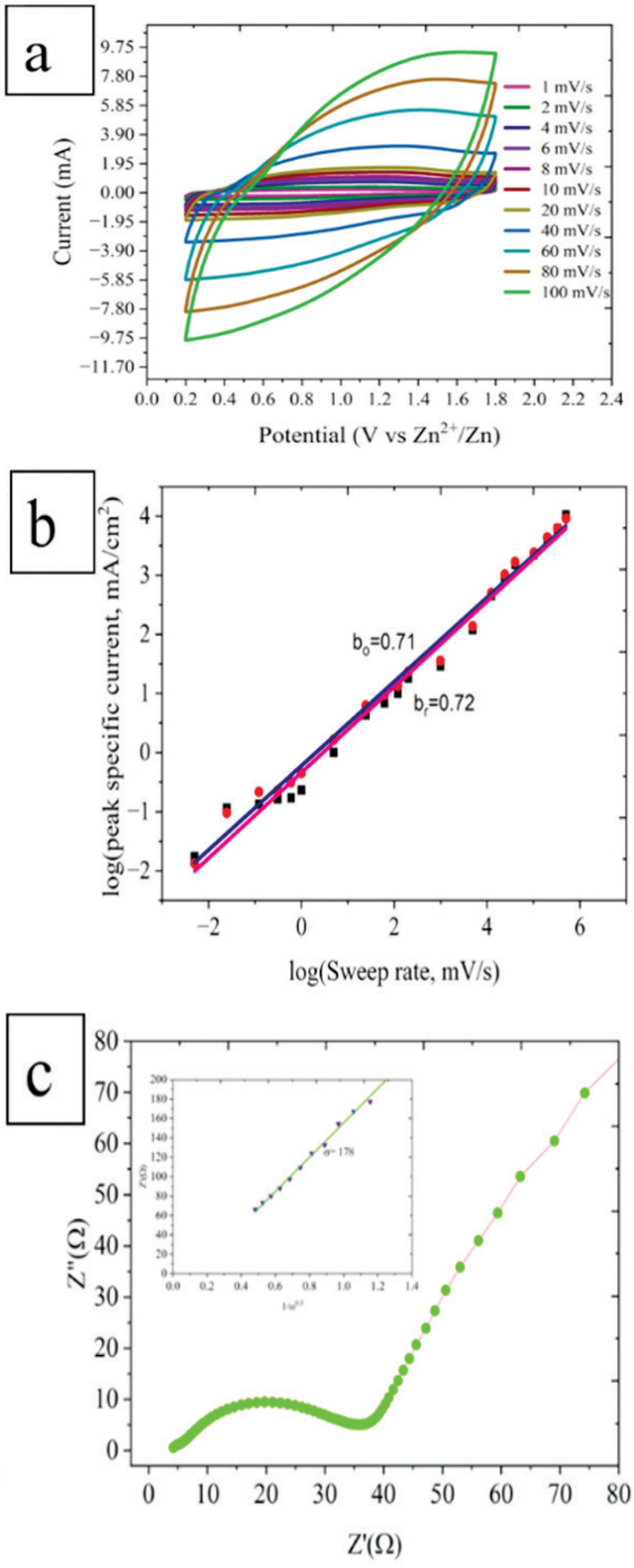


Fig. 5. The illustration of Zn/HMPC hybrid supercapacitor

Fig. 6(a) shows the cyclic voltammogram obtained (CV) at various scan rates ranging from 1 to 350 mV s^{-1} in the potential window of 0.2-1.8 V. The quasi- rectangular shape of the CV curve suggests the combined contribution of both capacitive and diffusion storage mechanism. The relation between the current and the scan rate was described by using equation, $i = av^b$, where i is the current, v is the scan rate, a and b are the adjustable parameters[47]. The value of b ranges from 0-1. Fig. 6(b) show the log i (current) versus log v (scan rate) plot for HPCM sample at oxidation and reduction peaks which is resulted from CV. The obtained values for b_o (oxidation process) and b_r (reduction process) for HPCM are 0.71 and 0.72, respectively. According to the previous studies, b=0.5 stands for diffusion (intercalation) controlled process, while b=1 shows

capacitive process. Hence, it confirms that our study indicates that the catalyst exhibits capacitive as well as diffusion process which plays an important role in the storing capacity. Fig. 6(c) shows EIS study,



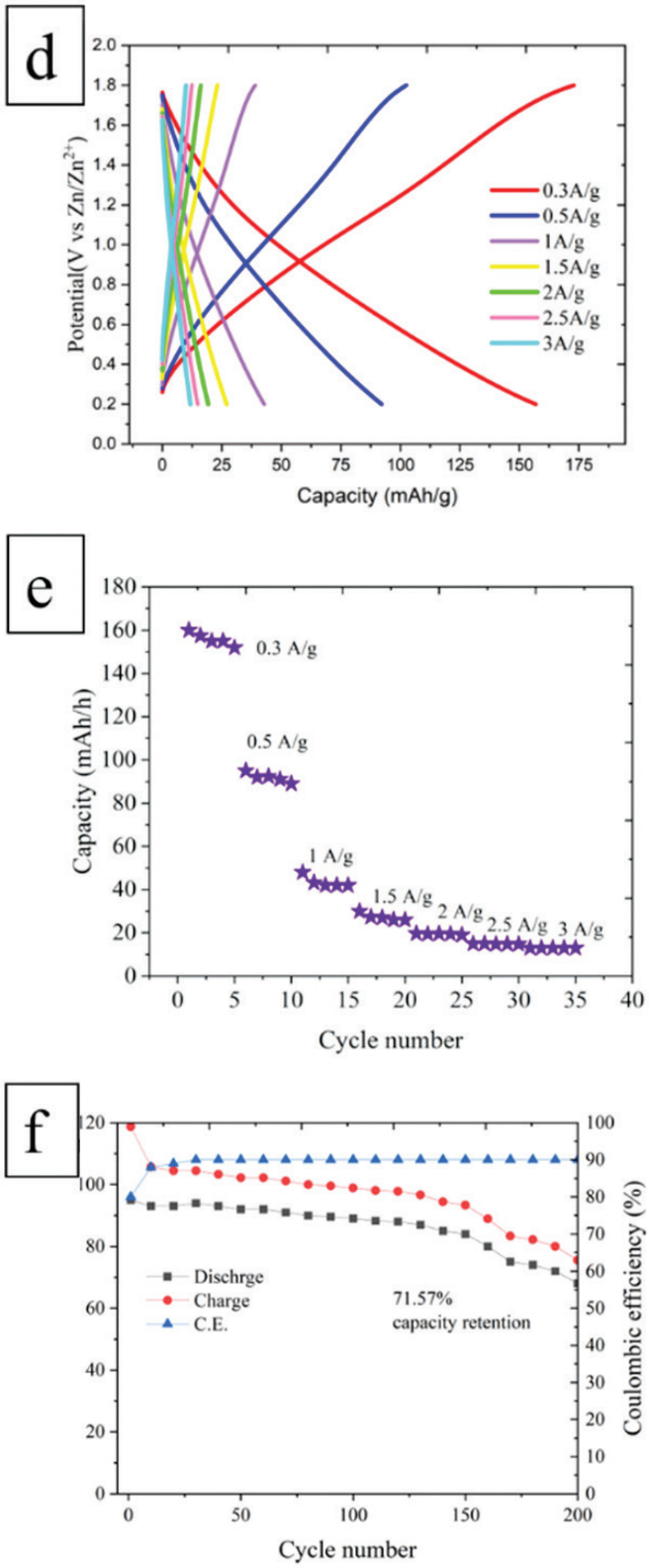


Fig. 6:a)Cyclic voltammogram for HPCM at scan of 1-100 mV/s, b) b-value, c) Nyquist plot, d) charge-discharge at various current densities, e) rate stability, f) cycling stability for HPCM as positive electrode for ZBHSC.

R_s represents the solution resistance, Rct indicates the charge-transfer resistance at the interfaces, and Z_w denotes the Warburg impedance associated to the diffusion of Zn^{2+} ions in equivalent circuit diagram. The Rct value for the HPCM is 26.32 Ω, Rs value is 3.68 Ω, and Z_w value is 178.

Fig. 6(d), display the charge/discharge curves of the HPCM based ZBHSC for the range of current densities from 0.3 to 3 A g^{-1} over the potential window of 0.2-1.8 V. The specific capacity obtained from charge-discharge curve are displayed at different current densities (0.3 to 3 A g^{-1}) are shown in fig. 6(e). At lower current density like 0.3 A g^{-1}, HPCM electrodes exhibit discharge capacity of 157.44 mAh g^{-1}, as current density increases, capacity decreases to 92.13, 42.92, 27.34, 18.85, 15.03,11.76 mAh g^{-1} for current densities of 0.3, 0.4, 0.5, 1, 1.5, 2, 2.5, and 3 A/g, respectively. Further, in order to demonstrate stability HPCM electrodes were charge/discharge at 0.5 A/g for 200 cycles. HPLC shows the capacity retention of 71.57 % and coulombic efficiency of 90.17% (Fig. 6(f)) which confirms the electrochemical stability of HPLC as cathode for ZBHSC. The cell exhibits a peak energy density of 56 Wh/kg at a power density of 106 W/kg, indicating its capability to store substantial energy while delivering moderate power. Additionally, it achieves an exceptional power density of 1.07 kW/kg at an energy density of 4.18 Wh/kg, highlighting its ability to deliver high power output under conditions of lower energy storage. This combination of performance metrics underscores the zinc ion hybrid supercapacitor versatility in applications requiring both high energy storage and rapid energy delivery. The future work includes working on improving specific capacity, cycling stability and capacity retention. This can be achieved by activating carbon and incorporating additional functional group to enhance electrochemical performance of secondary waste derived Marigold carbon which would be used in future green and cost-effective electrochemical device for large-scale production.

4. Conclusions

Secondary marigold flowers waste was effectively transformed into porous carbons by HTC and pyrolysis processes. Due to dehydration and decarboxylation at a high pyrolysis temperature, all functional groups were eliminated after the reaction. After treatment SMW converted to HPCM used as positive electrode showed attractive capacity of 157.44 mAh g^{-1} at 0.3 A g^{-1}. The ZBSC designed using HPCM as positive electrode displayed attractive the capacity retention of 71.57 % and coulombic efficiency of 90.17% over 200 cycles. The developed ZBHSC demonstrates a remarkable balance between energy and power capabilities, achieving a peak energy density of 56 Wh/kg at 106 W/kg and an outstanding power density of 1.07 kW/kg at 4.18 Wh/kg, making it highly versatile for diverse energy storage applications.

Acknowledgments

The authors are thankful to the CSIR (SRF/ RA- 2023), AICTE-ADF 2019. We would also like to thank SAIF IIT, Bombay for Material Characterization.

References

[1] J. B. Goodenough, "Electrochemical energy storage in a sustainable modern society," 2014. doi: 10.1039/c3ee42613k.

[2] Q. Liu, H. Wang, C. Jiang, and Y. Tang, "Multi-ion strategies towards emerging rechargeable batteries with high performance," 2019. doi: 10.1016/j.ensm.2019.03.028.

[3] M. Armand and J. M. Tarascon, "Building better batteries," 2008. doi: 10.1038/451652a.

[4] B. Dunn, H. Kamath, and J. M. Tarascon, "Electrical energy storage for the grid: A battery of choices," 2011. doi: 10.1126/ science.1212741.

[5] D. Pakulski *et al.*, "Novel Keplerate type polyoxometalate-surfactant-graphene hybrids as advanced electrode materials for supercapacitors," *Energy Storage Mater*, vol. 17, 2019, doi: 10.1016/j.ensm.2018.11.012.

[6] G. Zhang, X. Ou, C. Cui, J. Ma, J. Yang, and Y. Tang, "High-Performance Cathode Based on Self-Templated 3D Porous Microcrystalline Carbon with Improved Anion Adsorption and Intercalation," *Adv Funct Mater*, vol. 29, no. 2, 2019, doi: 10.1002/adfm.201806722.

[7] C. Jiang *et al.*, "A Multi-Ion Strategy towards Rechargeable Sodium-Ion Full Batteries with High Working Voltage and Rate Capability," *Angewandte Chemie - International Edition*, vol. 57, no. 50, 2018, doi: 10.1002/anie.201810575.

[8] J. Li, F. Hong, R. Xie, and P. Cheng, "Pore scale simulation of evaporation in a porous wick of a loop heat pipe flat evaporator using Lattice Boltzmann method," *International Communications in Heat and Mass Transfer*, vol. 102, 2019, doi: 10.1016/j.icheatmasstransfer.2019.01.008.

[9] B. Li *et al.*, "Nitrogen-doped activated carbon for a high energy hybrid supercapacitor," *Energy Environ Sci*, vol. 9, no. 1, 2016, doi: 10.1039/c5ee03149d.

[10] V. Aravindan, J. Gnanaraj, Y. S. Lee, and S. Madhavi, "Insertion-type electrodes for nonaqueous Li-ion capacitors," 2014. doi: 10.1021/cr5000915.

[11] S. Fleischmann *et al.*, "High voltage asymmetric hybrid supercapacitors using lithium- and sodium-containing ionic liquids," *Energy Storage Mater*, vol. 16, 2019, doi: 10.1016/j.ensm.2018.06.011.

[12] F. Wang *et al.*, "Highly reversible zinc metal anode for aqueous batteries," *Nat Mater*, 2018, doi: 10.1038/s41563-018-0063-z.

[13] R. J. Gummow, G. Vamvounis, M. B. Kannan, and Y. He, "Calcium-Ion Batteries: Current State-of-the-Art and Future Perspectives," 2018. doi: 10.1002/adma.201801702.

[14] H. Wang, Z. Wang, P. Bai, S. Hu, Y. Zhang, and R. Wang, "Optimized segmented heat source for the numerical simulation of welding-induced deformation in large structures," *Advances in Engineering Software*, vol. 117, 2018, doi: 10.1016/j.advengsoft.2017.12.005.

[15] L. Dong *et al.*, "Extremely safe, high-rate and ultralong-life zinc-ion hybrid supercapacitors," *Energy Storage Mater*, vol. 13, 2018, doi: 10.1016/j.ensm.2018.01.003.

[16] J. Hao *et al.*, "Toward High-Performance Hybrid Zn-Based Batteries via Deeply Understanding Their Mechanism and Using Electrolyte Additive," *Adv Funct Mater*, vol. 29, no. 34, 2019, doi: 10.1002/adfm.201903605.

[17] X. Dai, F. Wan, L. Zhang, H. Cao, and Z. Niu, "Freestanding graphene/VO2 composite films for highly stable aqueous Zn-ion batteries with superior rate performance," *Energy Storage Mater*, vol. 17, 2019, doi: 10.1016/j.ensm.2018.07.022.

[18] G. G. Yadav *et al.*, "Understanding the Effect of Zinc and Achieving Long Cycle Life in Cu-Intercalated Bi-Birnessite/Zinc Batteries," *ECS Meeting Abstracts*, vol. MA2017-02, no. 2, 2017, doi: 10.1149/ma2017-02/2/171.

[19] X. Zeng, J. Hao, Z. Wang, J. Mao, and Z. Guo, "Recent progress and perspectives on aqueous Zn-based rechargeable batteries with mild aqueous electrolytes," 2019. doi: 10.1016/j.ensm.2019.04.022.

[20] . S. and S. Choudhary, "REVIEW PAPER ON -ECOFRIENDLY PRACTICE IN TEMPLE TO MAKE SUSTAINABLE APPROACH TOWARD SOCIAL AND ENVIRONMENT," *International Journal of Technical Research & Science*, vol. 6, no. VI, 2021, doi: 10.30780/ijtrs.v06.i06.002.

[21] A. Sharma *et al.*, "Insights into rapid composting of paddy straw augmented with efficient microorganism consortium," *International Journal of Recycling of Organic Waste in Agriculture*, vol. 3, no. 2, 2014, doi: 10.1007/s40093-014-0054-2.

[22] M. S. Waghmode, A. B. Gunjal, N. N. Nawani, and N. N. Patil, "Management of Floral Waste by Conversion to Value-Added Products and Their Other Applications," 2018. doi: 10.1007/s12649-016-9763-2.

[23] M. B. Kulkarni and P. M. Ghanegaonkar, "Methane enrichment of biogas produced from floral waste: A potential energy source for rural India," *Energy Sources, Part A: Recovery, Utilization and Environmental Effects*, vol. 41, no. 22, 2019, doi: 10.1080/15567036.2019.1571126.

[24] S. Kumari, R. Kothari, V. Kumar, P. Kumar, and V. v. Tyagi, "Kinetic assessment of aerobic composting of flower waste generated from temple in Jammu, India: a lab-scale experimental study," *Environmental Sustainability*, vol. 4, no. 2, 2021, doi: 10.1007/s42398-021-00179-5.

[25] F. H. Isikgor and C. R. Becer, "Lignocellulosic biomass: a sustainable platform for the production of bio-based chemicals and polymers," *Polym Chem*, vol. 6, no. 25, 2015, doi: 10.1039/c5py00263j.

[26] N. Mohamad Nor, L. C. Lau, K. T. Lee, and A. R. Mohamed, "Synthesis of activated carbon from lignocellulosic biomass and its applications in air pollution control - A review," 2013. doi: 10.1016/j.jece.2013.09.017.

[27] J. Wang *et al.*, "Biomass derived carbon for energy storage devices," 2017. doi: 10.1039/c6ta08742f.

[28] L. Wang and X. Hu, "Recent Advances in Porous Carbon Materials for Electrochemical Energy Storage," 2018. doi: 10.1002/asia.201800553.

[29] Z. Yang *et al.*, "Recent Advancement of Nanostructured Carbon for Energy Applications," 2015. doi: 10.1021/cr5006217.

[30] A. M. Abioye and F. N. Ani, "Recent development in the production of activated carbon electrodes from agricultural waste biomass for supercapacitors: A review," 2015. doi: 10.1016/j.rser.2015.07.129.

[31] Y. Jin, K. Tian, L. Wei, X. Zhang, and X. Guo, "Hierarchical porous microspheres of activated carbon with a high surface area from spores for electrochemical double-layer capacitors," *J Mater Chem A Mater*, vol. 4, no. 41, 2016, doi: 10.1039/c6ta05872h.

[32] W. Xing *et al.*, "Superior CO2 uptake of N-doped activated carbon through hydrogen-bonding interaction," *Energy Environ Sci*, vol. 5, no. 6, 2012, doi: 10.1039/c2ee21653a.

[33] Y. S. Yun *et al.*, "Microporous carbon nanoplates from regenerated silk proteins for supercapacitors," *Advanced Materials*, 2013, doi: 10.1002/adma.201204692.

[34] R. J. Mo *et al.*, "Activated carbon from nitrogen rich watermelon rind for high-performance supercapacitors," *RSC Adv*, 2016, doi: 10.1039/c6ra10719b.

[35] H. Wang *et al.*, "Interconnected carbon nanosheets derived from hemp for ultrafast supercapacitors with high energy," *ACS Nano*, 2013, doi: 10.1021/nn400731g.

[36] D. Bhattacharjya and J. S. Yu, "Activated carbon made from cow dung as electrode material for electrochemical double layer capacitor," *J Power Sources*, vol. 262, 2014, doi: 10.1016/j.jpowsour.2014.03.143.

[37] A. M. Abioye, Z. A. Noorden, and F. N. Ani, "Synthesis and Characterizations of Electroless Oil Palm Shell Based-Activated Carbon/Nickel Oxide Nanocomposite Electrodes for Supercapacitor Applications," *Electrochim Acta*, 2017, doi: 10.1016/j.electacta.2016.12.101.

[38] M. Wahid, G. Parte, D. Phase, and S. Ogale, "Yogurt: A novel precursor for heavily nitrogen doped supercapacitor carbon," *J Mater Chem A Mater*, 2015, doi: 10.1039/c4ta06068g.

[39] Z. Li *et al.*, "Carbonized chicken eggshell membranes with 3D architectures as high-performance electrode materials for supercapacitors," *Adv Energy Mater*, 2012, doi: 10.1002/aenm.201100548.

[40] T. E. Rufford, D. Hulicova-Jurcakova, Z. Zhu, and G. Q. Lu, "Nanoporous carbon electrode from waste coffee beans for high performance supercapacitors," *Electrochem commun*, 2008, doi: 10.1016/j.elecom.2008.08.022.

[41] W. Qian *et al.*, "Human hair-derived carbon flakes for electrochemical supercapacitors," *Energy Environ Sci*, 2014, doi: 10.1039/c3ee43111h.

[42] B. Hu, K. Wang, L. Wu, S. H. Yu, M. Antonietti, and M. M. Titirici, "Engineering carbon materials from the hydrothermal carbonization process of biomass," 2010. doi: 10.1002/adma.200902812.

[43] S. K. Hoekman, A. Broch, and C. Robbins, "Hydrothermal carbonization (HTC) of lignocellulosic biomass," *Energy and Fuels*, vol. 25, no. 4, 2011, doi: 10.1021/ef101745n.

[44] N. Chaiammart, S. Wongcharoen, A. Eiad-Ua, T. Ishizaki, and G. Panomsuwan, "Transformation of waste marigold flowers into porous carbons via hydrothermal carbonization," in *Key Engineering Materials*, 2019. doi: 10.4028/www.scientific.net/KEM.824.23.

[45] Z. Xie, W. Guan, F. Ji, Z. Song, and Y. Zhao, "Production of biologically activated carbon from orange peel and landfill leachate subsequent treatment technology," *J Chem*, vol. 2014, 2014, doi: 10.1155/2014/491912.

[46] S. Sonal, P. Prakash, B. K. Mishra, and G. C. Nayak, "Synthesis, characterization and sorption studies of a zirconium(IV) impregnated highly functionalized mesoporous actIVated carbonsb," *RSC Adv*, vol. 10, no. 23, 2020, doi: 10.1039/c9ra10103a.

[47] S. Khamsanga, R. Pornprasertsuk, T. Yonezawa, A. A. Mohamad, and S. Kheawhom, "δ-MnO2 nanoflower/graphite cathode for rechargeable aqueous zinc ion batteries," *Sci Rep*, vol. 9, no. 1, pp. 1–9, 2019, doi: 10.1038/s41598-019-44915-8.